Stability and switching in whispering-gallery-mode microdisk lasers

A. Eschmann and C. W. Gardiner
Physics Department, University of Waikato, Hamilton, New Zealand
(Received 6 July 1993; revised manuscript received 4 October 1993)

We examine whispering-gallery-mode microdisk lasers, which have some potential for use in optical computing, in an attempt to determine their stability and switching properties. We solve the laser equations for a coupled-laser system and investigate the stability and switching properties of these solutions. We find that the lasers are stable and switch reliably in the absence of noise. If reasonable estimates of noise are included, spontaneous switching rates of the order of once a year can be arranged using physically reasonable parameter values.

PACS number(s): 42.60.−v

I. INTRODUCTION

Recently, lasers of a novel structure named whispering-gallery-mode microdisk lasers were created [1]. Current investigations are under way for the possibility of fabrication of these lasers for use in photonic or optoelectronic circuits [2,3].

A schematic in Fig. 1 shows the structure of the laser and the way in which light propagates in the laser. These lasers may be coupled together via dielectric material as shown in Fig. 2. Waves propagating outward from the disk into the surroundings dielectric, which has a low refractive index compared with the laser, are evanescent out to a certain radius, where they tunnel through an angular-momentum potential barrier. Beyond this the waves propagate freely outwards from the disk. Such a coupling scheme is a useful one as it allows these semiconductor lasers to be arranged in large monolithic arrays, and thus enhances their potential for usage in optical or optoelectronic systems.

For such small lasers, the effects of quantum noise become important, hence stability and reliable switching capabilities must be ensured, and the aim of this paper is to investigate whether these lasers have reliable stability and switching properties.

We do this using two theoretical models. The first model uses a simple gas-laser saturation function in order to avoid complex dependences on the semiconductor band structure. The majority of our results are obtained using this model. The second model uses a more realistic semiconductor saturation function which includes the effect of refractive-index saturation and frequency pulling. Results using this model are included as a check on the validity of the results of the simplified model. These models are discussed in more detail in Sec. II.

We solve the laser equations for a system composed of two coupled lasers (as shown in Fig. 2), which exhibit bistability—the stable solutions correspond to the lasers being either in phase or in antiphase. Because rigid monolithic arrays of these lasers can be made, the use of phase as an information element is feasible. In Sec. III we investigate the switching and stability of these solutions in the absence of noise. In Sec. IV the stability of the bistable system against fluctuations is investigated numerically, using reasonable values of the parameters. It is found that spontaneous switching rates of the order of a year might occur.

II. EQUATIONS FOR COUPLED LASERS

The high index contrast ratio between a whispering-gallery-mode microdisk laser and its surroundings means that the lasers have high-Q values. This enhances the reflectivity and mode selectivity of the microcavity, and hence it is valid to adiabatically eliminate all variables except the field mode. Our coupling is therefore between two single-mode lasers. This is in contrast to the usual situation for semiconductors, in which it is not possible

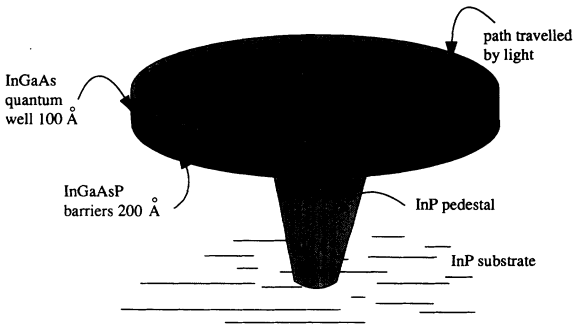

FIG. 1. Whispering-gallery-mode microdisk laser.

FIG. 2. Microdisks coupled together via dielectric material. The coupling strength can be engineered by varying the length and type of coupling material, and the gap between the coupling material and the laser [9]. Diffracton gratings can also be used to couple light out of the disks [3].

to eliminate all modes but the field because the cavity mirrors are simply the end faces of the cavity itself and the semiconductor is therefore low Q.

This coupling between the two lasers is brought about by introducing dielectric material to connect the lasers. Photons can then tunnel out from one laser and propagate freely into the second laser as described in Sec. I.

We use two different saturation functions to obtain results. The first of these is the gas-laser saturation function which has the form

$$f(|\alpha|^2)=\frac{\kappa C}{1+\frac{|\alpha|^2}{n_0}} , \tag{1}$$

where C is the cooperativity parameter, κ the decay constant for photons from the mode, n_0 is the saturation photon number, and α is the c number corresponding to the photon annihilation operator for the mode at frequency ω. This is much simpler than the actual saturation function, which has a complex dependence on the band structure of the semiconductor. The behavior of the gas-laser saturation function is rather different from that of the semiconductor saturation function [4], however we hope that the same qualitative results may be obtained.

The validity of using the gas-laser saturation function is tested by obtaining some results using a semiconductor laser saturation function. This saturation function is modeled on an ensemble of two-level atoms with a distribution of transition frequencies determined by the density of states [5]. It has the form

$$f(|\alpha|^2)=\kappa\left[\frac{C'\left(1-i\beta\sqrt{1+\frac{|\alpha|^2}{n_0}}\right)\frac{|\alpha|^2}{n_0}}{\sqrt{1+\frac{|\alpha|^2}{n_0}}\left(1+\sqrt{1+\frac{|\alpha|^2}{n_0}}\right)}+C''\right] , \tag{2}$$

where C' and C'' are coefficients chosen so that the two models have the same behavior for small $|\alpha|^2$ and $\beta=0$, and β is a dimensionless parameter dependent on the band structure of the semiconductor. The size of β determines the size of the refractive index, and the frequency shift of the laser. The sign of β determines the direction of the frequency shift and if $\beta=0$ no frequency shift occurs. This refractive-index saturation which leads to the frequency shift of the lasing mode is not found in the gas-laser model.

The laser equation for a single microlaser resonant for a single mode may be obtained from the appropriate Hamiltonian [6]. Thus we can write, in a frame rotating at the laser frequency,

$$\dot{\alpha}=-\kappa\alpha+\alpha f(|\alpha|^2)+\xi(t) , \tag{3}$$

where $\xi(t)$ is a Gaussian noise term whose only nonzero correlation is

$$\langle\xi^*(t)\xi(t')\rangle=2Q(\alpha)\delta(t-t') . \tag{4}$$

The value of $Q(\alpha)$ will be discussed later.

The equations for two coupled single-mode lasers can be obtained from (3) by including a coupling term between the modes of each laser which comes about from the additional Hamiltonian term

$$H_{\text{coupling}}=\hbar\epsilon(a_1^\dagger a_2+a_2^\dagger a_1) . \tag{5}$$

Hence the laser equations for the coupled system are

$$\dot{\alpha}_1=-\kappa_1\alpha_1+\alpha_1 f_1(|\alpha_1|^2)-i\epsilon\alpha_2+\xi_1(t) , \tag{6}$$

$$\dot{\alpha}_2=-\kappa_2\alpha_2+\alpha_2 f_2(|\alpha_2|^2)-i\epsilon\alpha_1+\xi_2(t) . \tag{7}$$

An idea of the types of solution we may expect can be obtained by considering the deterministic equations, using the gas-laser saturation function, in the situation in which $C_1=C_2$ and $\kappa_1=\kappa_2$. In this situation there exist parameters for which

$$\left[1-\frac{C}{1+\frac{|\alpha_1|^2}{n_0}}\right]=\left[1-\frac{C}{1+\frac{|\alpha_2|^2}{n_0}}\right]=0 . \tag{8}$$

This leads to two sets of solutions of Eqs. (6) and (7) which correspond to two different physical states. These are the antisymmetric state

$$\alpha_1=re^{i\epsilon t} , \quad \alpha_2=-re^{i\epsilon t} , \tag{9}$$

and the symmetric state

$$\alpha_1=ae^{-i\epsilon t} , \quad \alpha_2=ae^{-i\epsilon t} . \tag{10}$$

Thus for identical lasers we would expect the system to evolve into the states given in (9) and (10), that is, in-phase states oscillating at frequency $-\epsilon$, and out-of-phase states oscillating at frequency ϵ. Numerical investigations show that this qualitative behavior is present even when $C_1\neq C_2$ and $\kappa_1\neq\kappa_2$ provided they are not too different. These two sets of solutions may be used to represent the binary digits 0 and 1 which are used in optical computing.

There are two principal requirements of a logic element: we must be able to change states when desired; the system must remain in a given configuration until a change in configuration is desired.

We expect the latter to be true on a macroscopic scale where the effects of quantum noise are small, but on the scale we consider, which is of the order of micrometers, the quantum effects may become significant and cause switching to occur. In the next section we investigate the switching of deterministic solutions, and in the following section consider to what extent noise may induce spontaneous switching.

III. DETERMINISTIC SIMULATIONS

Initial simulations of the deterministic versions of Eqs. (6) and (7) were performed using the gas-laser saturation function, to ensure that the system did indeed display the predicted stability and that the system could be made to switch. The following parameter sizes were used.

(1) $\epsilon=2.1\times10^{13}$ s^{-1}. This is the weakest coupling strength for which we found stability to be obtained, given a slight detuning as discussed below.

(2) We allow for manufacturing differences and hence slightly detune the values of κ_1 and κ_2. These values are taken as $\kappa_1+(2.1+i0.1)\times10^{13}$ s^{-1} and $\kappa_2=2\times10^{13}$ s^{-1}.

(3) We take $C_1\sim C_2\sim5$, which suggests that we operate well above threshold within the gain region.

(4) We choose n_0 to be 100. The qualitative behavior of the system is unaffected by this choice and we take this value for the sake of consistency with later simulations. Some simulations were also run using the semiconductor saturation function for which the following additional parameters were used.

(a) As mentioned previously, C_1', C_2', C_1'', and C_2'' are chosen so that the gas-laser saturation function is obtained in the limit of small $|\alpha_i|^2/n_0$ when $\beta=0$. In other words $C_i'=-2C_i$ and $C_i''=C_i$ where $i=1,2$.

(b) We have chosen β to be 0.1. The larger the value of β the larger the frequency shift of the laser. Eventually this destroys the desired bistability effect, which is required for optical computing. The value we have chosen is large enough to show the effect of refractive-index saturation in the semiconductor laser saturation function in our analysis. In practice, it is expected that the value of β could be determined by appropriate engineering [7].

A. Stability

To test stability we used random initial conditions, simulated the system's evolution, and then checked to see which final state the laser system evolved into. We expect that the system will evolve into the state closest to the initial state. By this we mean that for an initial phase difference between the modes of $-\pi/2<\phi<\pi/2$ the system will evolve into the symmetric final state, which has a final phase of zero, and for $\pi/2<\phi<3\pi/2$ the system goes to an antisymmetric final state, with a phase difference of π. We carried out several runs, each time using different random amplitude r and phase ϕ values

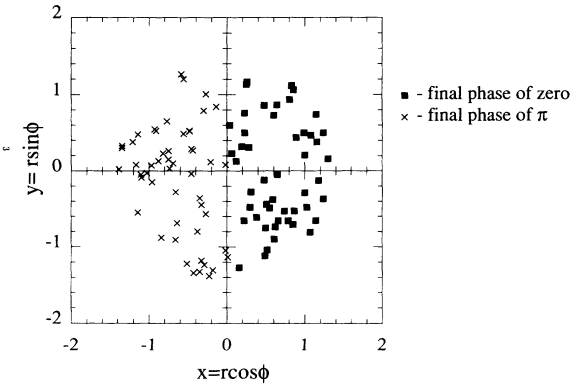

FIG. 3. Phase-space distribution of initial points showing final states into which they evolve for the gas-laser saturation function. The squares represent a final phase of zero, and the crosses a final phase of π. The figure shows that initial phases of ϕ which satisfy $\pi/2<\phi<\pi/2$ lead to a final state of 0, with a corresponding result for $\pi/2<\phi<3\pi/2$.

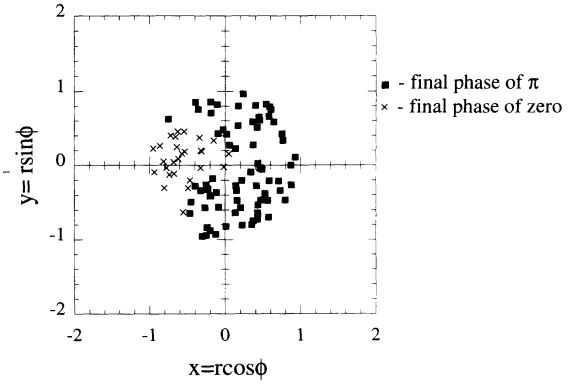

FIG. 4. Phase-space distribution of initial points showing final states into which they evolve using the semiconductor saturation function with $\beta=0.1$. The squares represent a final phase of zero, and the crosses a final phase of π. The size of the wedge decreases with increasing β.

for $\alpha_0(2)=re^{i\phi}$, while fixing $\alpha_0(1)$ to be 1. The results are shown in Fig. 3 for the gas-laser saturation function. From this we can see that the prediction that the system is bistable is correct and that for the system in a given initial state, the final state can be predicted and is one of the states given by the solution of the laser equations.

Figure 4 shows similar data where the semiconductor laser saturation function has been used for $\beta=0.1$. It can be seen that two distinct final states are still obtained, however the in-phase final state is preferred over the out-of-phase final state. For $\beta=-0.1$ the converse is true. For larger β the wedge of out-of-phase final values becomes smaller and eventually disappears altogether for $\beta=0.24$. We thus conclude that provided β is not too large a useful bistability behavior still exists. The prediction that the system will evolve into the state closest to the initial state is clearly no longer valid for this choice of parameters. It should be pointed out, however, that the wedge size can be increased by increasing the value of ϵ, the coupling strength. Hence by careful choice of ϵ, the size of the effect of β can be controlled.

B. Switching

We would like to be able to switch the state of the laser reliably when desired. This can be brought about by applying a pulse to each laser in the coupled system.

If we have an initially symmetric state, the pulse must be applied to each laser antisymmetrically; i.e., the pulse must be applied with opposite phases to each laser, for a phase change to take place and for antisymmetry to result. If the pulse is applied symmetrically, i.e., with the same phase to each laser, the symmetry is being reinforced, and no switch will occur. Conversely, if we have an antisymmetric state initially, the pulse must be applied to each laser symmetrically for a switch to the symmetric state to take place. We examine three kinds of pulse.

(1) A pulse in which the amplitude and phase are constant throughout the duration of the pulse. We call this the zero-frequency pulse.

(2) A pulse with a phase varying with the field-mode

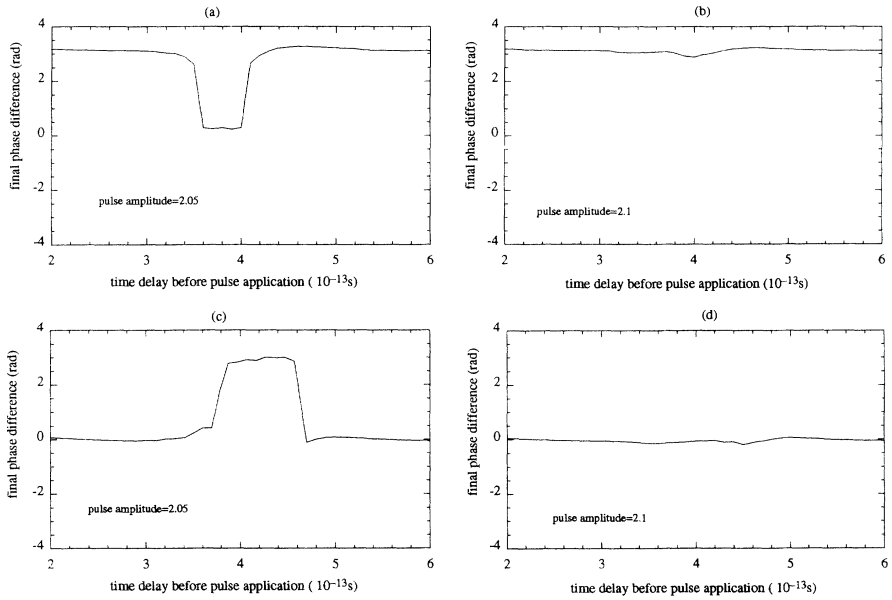

FIG. 5. (a) and (b) Unstable and stable switching for initially symmetric states for a zero-frequency pulse applied antisymmetrically. (c) and (d) Unstable and stable switching for initially antisymmetric states for a zero-frequency pulse applied symmetrically.

frequency ϵ, which we shall call a positive-frequency pulse. Such a pulse will be in resonance with the frequency of the antisymmetric state.

(3) A pulse with a phase varying with the field-mode frequency $-\epsilon$, which we shall call a negative-frequency pulse. Such a pulse will be in resonance with the frequency of the symmetric state.

We apply the pulse for at least as long as $2\pi/\epsilon$. We wish to ensure that a stable switch will occur to the final state, given that a pulse can be applied at any point in the oscillation cycle of the field. We thus consider a pulse applied at various points throughout one oscillation cycle of the field, and our graphs therefore display the final state obtained for a given pulse delay. We consider the results for the case of the gas-laser saturation function.

For application of a zero-frequency pulse in the case of finite pulse duration similar switching amplitudes (by this we mean the minimum amplitude which gives reliable switching) are obtained for switching from symmetric to antisymmetric states and antisymmetric to symmetric states. This is shown in Fig. 5. This is expected, as the pulse which is applied has a frequency which is the average of the positive and negative frequencies and hence one pulse is not preferred over the other. The slight discrepancy arises as a result of the slight detuning in the decay constants.

For the positive-frequency pulse, entirely different results are expected depending on our initial state since this frequency is the same as that of the antisymmetric state. Because we have a positive-frequency pulse, we expect that it will be easier to drive the system into an antisymmetric final state in which the modes also have a positive frequency, and harder to drive the system into a symmetric state in which the modes have the opposite fre-

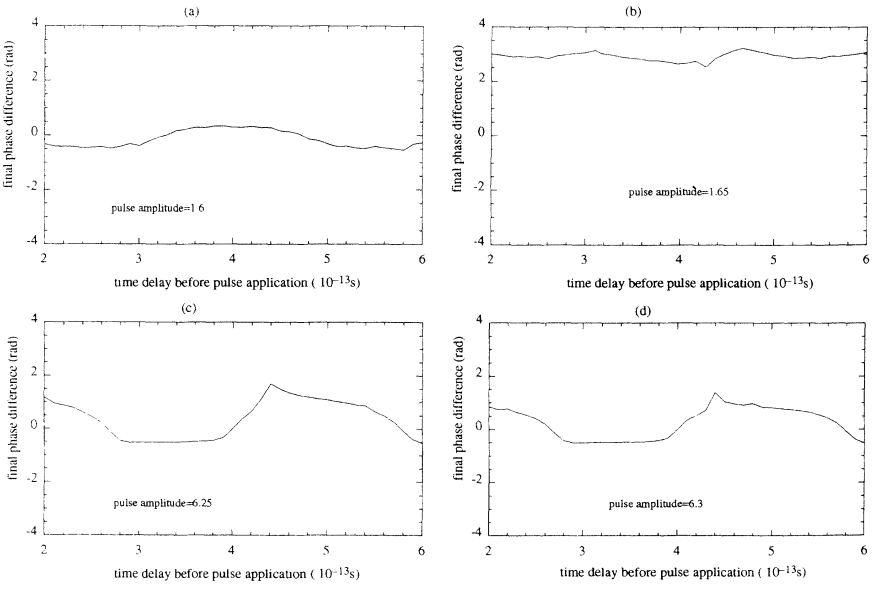

FIG. 6. (a) and (b) Unstable and stable switching for intially symmetric states for a positive-frequency pulse applied antisymmetrically. (c) and (d) Unstable and stable switching for initially antisymmetric states for a positive-frequency pulse applied symmetrically.

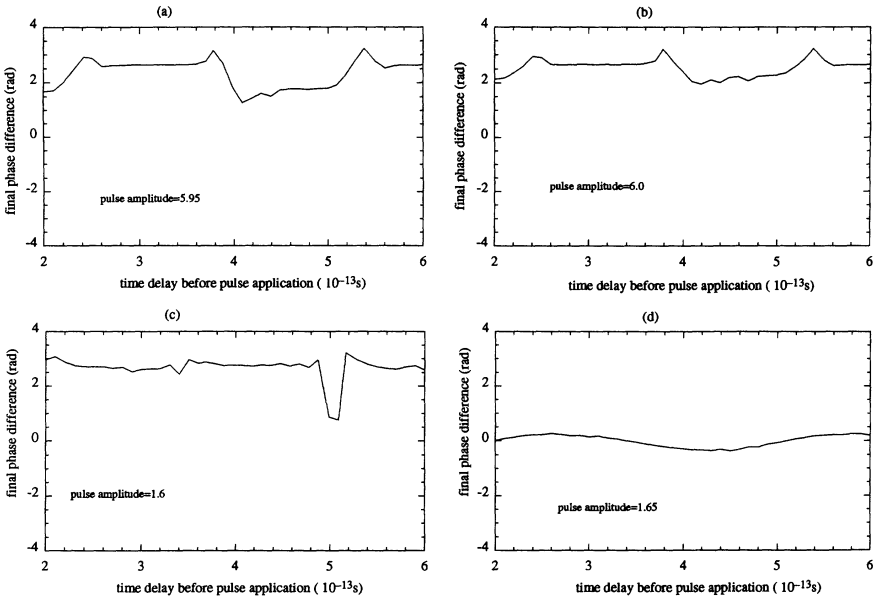

FIG. 7. (a) and (b) Unstable and stable switching for initially symmetric states for a negative-frequency pulse applied antisymmetrically. (c) and (d) Unstable and stable switching for initially antisymmetric states for a negative-frequency pulse applied symmetrically.

quency. The results shown in Fig. 6 confirm this.

For the negative-frequency pulse we expect the opposite results to those obtained for the positive-frequency case. That is, a smaller amplitude is expected to be required to switch to the symmetric state than the antisymmetric state. Again, the results shown in Fig. 7 confirm this.

If a semiconductor saturation function is used it is found that for $\beta=0.1$, switching to the symmetric state is easier for all three pulse types. This is not surprising when one recalls that in Fig. 4 the in-phase final state is preferred. Stable switching to the antisymmetric state is also possible but for pulse amplitudes which are $\sim 1.5-3$ times higher than those for switching from antisymmetric to symmetric states.

For the above results we have taken a pulse length of the order of the period of the field modes, however, another choice of pulse length may facilitate switching in certain cases. Hence we consider the effect of pulse length on ease of switching. To do this we have applied a very long pulse in each of the three pulse cases to see whether switching is enhanced or inhibited.

We find that resonance effects become important. For the zero-frequency case, we find that the required switching amplitudes are decreased as the step provides a continual drive into the final state. For the positive-frequency case however, resonance effects mean that switching from antisymmetric to symmetric states is impossible whereas switching from symmetric to antisymmetric states is enhanced. For the negative-frequency case the opposite results are obtained. That is, switching from symmetric to antisymmetric states is impossible.

We have also examined the effects of varying the detuning and the damping on our system. This must be done as no two lasers are the same, and reflectivities will vary from device to device. We vary the amount of detuning by varying imaginary parts of one of the decay constants κ_1, and the damping by varying the real parts of κ_1. The results are presented in Fig. 8 for switching from antisymmetric to symmetric states. We see that there is a definite boundary between stability and instability in each case, and that the boundary occurs in different positions of the graph for each pulse type. We see that for the negative-frequency pulse case more detuning and damping can be tolerated than for the zero-frequency pulse case, which in tern can tolerate more than the positive-frequency pulse case. This corresponds to the previous results where switching from antisymmetric to symmetric states required much smaller pulse amplitudes for the negative frequency than the positive frequency. For these results we have used the minimum pulse amplitudes for which stable switching was obtained in the previous analyses, however unstable switching can be overcome if higher pulse amplitudes are used. For switching from symmetric states to antisymmetric states the opposite results to those above are found i.e., the positive-frequency case is able to tolerate more detuning.

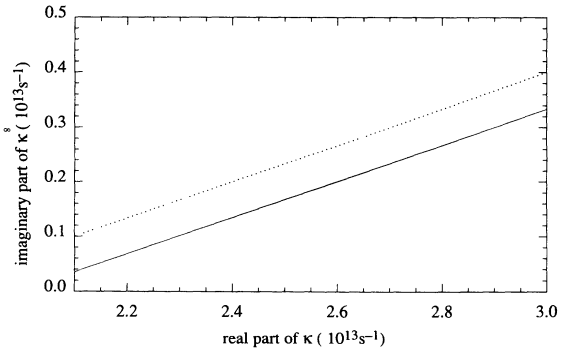

FIG. 8. Effects of varying the detuning and damping for switching from antisymmetric to symmetric states. Stable switching occurs for all three pulse types in the region below the solid line. In the region between the dotted and solid lines, the postive-frequency pulse ceases to switch in a stable manner, and above the dotted line, only the negative-frequency pulse case gives reliable switching.

IV. EFFECTS OF NOISE ON STABILITY

We now consider the effects of quantum noise on this system to see how long it takes for a spontaneous switch to occur and to examine whether this is long enough for optical storage to be feasible using this system. We include noise terms in our equations and perform numerical simulations. These simulations have been carried out using the gas-laser saturation function.

The integration scheme used for the simulations is the implicit stochastic method [8]. We use the following parameter sizes in the simulation, which are calculated from parameters given in [1].

(1) The inverse cavity lifetime κ is found from

$$Q=\frac{2\pi\nu_0}{\kappa} ,$$

where an approximate figure for Q is 200×10^{13} s^{-1} [1], and ν_0 can be calculated from the lasing wavelength which is 1.3 μm.

(2) The value of C depends in a complex manner on the pumping. A value of C of 1 represents threshold. We wish to work well in the gain region, thus we choose a value of C of ~5 as before.

(3) n_0, which is the approximate saturation photon number for the system, is 100 [9].

(4) ϵ be assigned arbitrarily, but in reality we expect it to be of the order of the decay constant. We selected a value of 0.01×10^{13} s^{-1} for the purposes of short computer runs when examining the effect of noise size on switching time.

(5) The noise size can be calculated from the spectral properties of the lased light and from the equation [6]

$$\tau=\frac{2n_0(C-1)}{Q(\alpha)} , \tag{11}$$

where τ is the phase correlation time $\tau=2\pi/\delta\omega$. We find a maximum $Q(\alpha)$ of 1.72×10^{13} s^{-1}. This upper bound is determined by the limited resolution of the spectrometer used to find the spectral linewidth.

Two sets of simulations are carried out. In the first of these the value of $Q(\alpha)$ is fixed and the effect of varying the coupling strength on the switching time is examined. The second simulation examines the effect of varying $Q(\alpha)$ on the switching time while ϵ remains fixed. The purpose of the simulations is to ascertain an average switching time at which the system spontaneously switches from one state to another. These simulations lead to two equations for the switching time as a function of ϵ and $Q(\alpha)$, which we compare.

Initially we examine the effect of coupling strength on switching time under the influence of the maximum theoretical amount of quantum noise as given above. For each value of the coupling strength, the simulation is run and several switching times are recorded. The switching times are averaged and graphs of ϵ vs average switching time t are produced. These results are shown in Fig. 9. The averages are performed over 50 switching times per ϵ value, and an exponential relationship between ϵ and t is found. From the lines of maximum and minimum slope in the figure we measure a mean slope of 25.5×10^{-13}

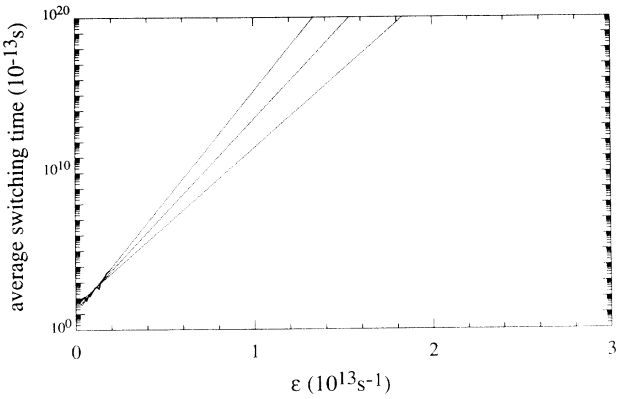

FIG. 9. Semilogarithmic plot and extrapolation of Eq. (12).

with an error of about 5%. A mean intercept value of 88.70×10^{13} s can also be obtained. We may thus write the expression for t

$$t=a\epsilon^{b\epsilon} \text{ s} , \tag{12}$$

where

$$a=88.70\times10^{-13} \text{ s} ,$$

$$b=25.54\times10^{-13} .$$

Substituting for $t=10^7$ s which would correspond to a storage time of the order of one year (1 year $=3.16\times10^7$ s), and ϵ value of 1.63×10^{13} s^{-1} is found, which is approximately twice the size of the decay constant.

To examine the effects of noise on the system, we have chosen an ϵ value of 0.01×10^{13} s^{-1}, as mentioned previously. The results are given in Fig. 10. The relationship found is an exponential one between t and Q^{-1}. We find from the lines of maximum and minimum slope in the figure a mean slope of 0.9835×10^{13} with an error of about 10%. A mean intercept value of 126.949×10^{-13} s can be found also. The slope is actually a constant multiplied by ϵ, therefore, removing ϵ from our slope value we obtain

$$t=ce^{d\epsilon/Q(\alpha)} \text{ s} , \tag{13}$$

where

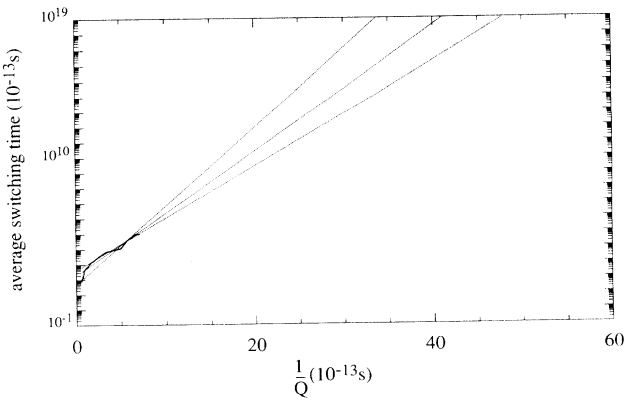

FIG. 10. Semilogarithmic plot and extrapolation of Eq. (13).

$$c = 126.949 \times 10^{13} \text{ s} ,$$

$$d = 98.35 .$$

Using a more realistic ϵ value of the order of the decay constant, $\epsilon = 0.7 \times 10^{13}$ s^{-1} in (13), and setting $t = 10^7$ s we find that $Q(\alpha) = 1.69 \times 10^{13}$ s^{-1} which is just below the theoretical maximum. The error in this value is about 10%. We can generalize (12) in a similar manner by removing $Q(\alpha)$ from the value for the slope. Then (12) becomes

$$t = ae^{f\epsilon/Q(\alpha)} \text{ s} , \tag{14}$$

where

$$f = 43.86 .$$

Then upon substituting in this new expression for $\epsilon = 0.7 \times 10^{13}$ s^{-1} we obtain $Q(\alpha) = 0.739 \times 10^{13}$ s^{-1}. This value has an error of approximately 5%. Thus the values of $Q(\alpha)$ obtained by the separate methods both fall below the theoretical maximum. Although approximate error estimates are given, these are not of great importance, as our results show that both simulations give results which have the same general behavior and both predict that switching times of one year are possible. These results seem promising for the semiconductor whispering-gallery-mode microdisk laser.

V. CONCLUSIONS

In conclusion we have shown that a bistable device can be devised and it can be made to switch in a stable manner. We have shown this to be true independently of the explicit laser model, provided that the value of β used is not too large. For the cases in which quantum noise is included in the system we predict that the microdisks are potentially stable over a time of the order of years, and hence may be useful in optical computing.

To further determine the usefulness of these lasers, a better estimate of the lasing linewidth is required. Another factor which may affect the results is the quality factor $Q(\alpha)$, for which we have only an approximate value, which determines the value of κ.

[1] S. L. McCall, A. F. J. Levi, R. E. Slusher, S. J. Pearton, and R. A. Logan, App. Phys. Lett. **60**, 289 (1992).
[2] A. F. J. Levi, R. E. Slusher, S. L. McCall, T. Tanbun-Ek, D. L. Coblentz, and S. J. Pearton, Electron. Lett. **28**, 101 (1992)
[3] A. F. J. Levi, R. E. Slusher, S. L. McCall, J. L. Glass, S. J. Pearton, and R. A. Logan, Appl. Phys. Lett. **62**, 561 (1993).
[4] G. P. Agrawal and N. K. Dutta, *Long Wavelength Semiconductor Lasers* (Van Nostrand Reinhold, New York, 1986).
[5] G. P. Agrawal, J. Appl. Phys. **63**, 1232 (1988).
[6] C. W. Gardiner, *Quantum Noise* (Springer-Verlag, Heidelberg, 1991).
[7] N. K. Dutta, N. A. Olssen, and W. T. Tang, Appl. Phys. Lett. **45**, 836 (1984).
[8] A. M. Smith and C. W. Gardiner, Phys. Rev. A **39**, 3511 (1989).
[9] R. E. Slusher (private communication).

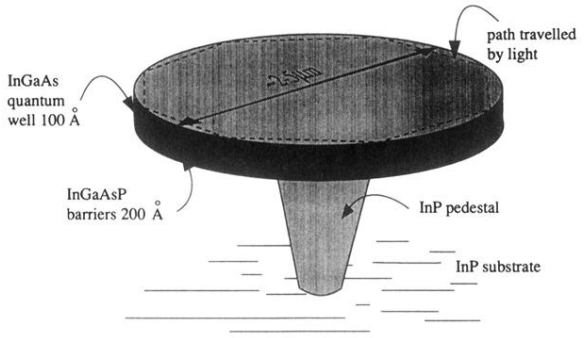

FIG. 1. Whispering-gallery-mode microdisk laser.

FIG. 2. Microdisks coupled together via dielectric material. The coupling strength can be engineered by varying the length and type of coupling material, and the gap between the coupling material and the laser [9]. Diffracton gratings can also be used to couple light out of the disks [3].